Deliverable #5: Final Report

EML4551C-Senior Design Fall 2013

Team 20- Direct Drive Solar-Powered Arcjet Thruster

Sponsor: Kurt Polzin (NASA)

Faculty Advisor: Wei Guo, Kwan Bing, Petru Andrei

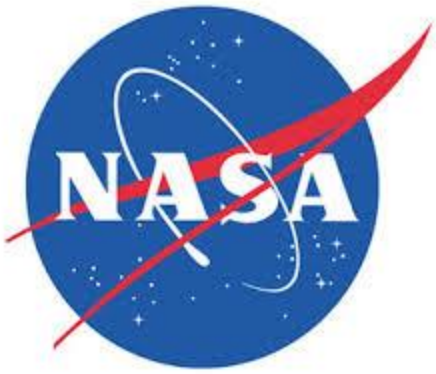

Group Members

Christopher Brolin

Cory Gainus

Gerard Melanson

Tara Newton

Griffin Valentich

Shane Warner

Table of Contents

1.0 Abstract

The importance of long term control of satellite and spacecraft systems provides an excellent opportunity for advancement in existing propulsion technologies. For the scope of this project, a solar powered arcjet thruster must be designed that eliminates the necessity of a power processing unit (PPU). Currently, startup of the thruster is achieved by transforming solar power to a desirable voltage and current via the PPU. Lighter, more affordable arcjet systems can be sent into space if this PPU is eliminated and, instead, directly driven by the solar panels. This increases the efficiency of the thruster as one of the components that fails most often is the PPU as a result of overheating. One topic under examination is the amount of thrust that can be generated without this PPU, in so-called "direct drive mode". Reduced cost of a system that provides low thrust but high specific impulse in this manner could greatly improve the functionality of thrusters used in space.

2.0 Acknowledgement

Special acknowledgements should be given to all of our faculty advisors as well as our sponsor Dr. Polzin of the NASA Marshall Space Flight Center for their support and feedback on various aspects of the project and the design process.

3.0 Project Overview

3.1 Customer/Sponsor Requirements:

- Produce a high voltage-pulse that can breakdown the injected gas to cause ionization.
- Design a scalable arcjet thruster capable of processing 50-400W of power without the use of a power processing unit.
- Design a vacuum chamber in order to properly simulate the space environment for testing the thruster.
- Design and execute a test/experiment in order to determine the thruster's range of operating conditions over which the ionization or gas breakdown will occur.
- Perform a successful test to quantify the conditions over which a continuous discharge at the given power levels can be sustained.
- Determine if this continuous discharge is possible within the range of conditions provided by the solar panels

3.2 Scope:

The project scope is to design, fabricate, and test an electric arcjet thruster within a vacuum chamber that will be designed to simulate the space environment at which the thruster will operate. The arcjet thruster will operate on a direct drive system eliminating the need for a power processing unit (PPU), thereby reducing the weight of the system, its complexity, and most importantly cost while maintaining efficiency. The use of solar panels as the arcjet's source of energy will be used since the abundance of solar energy is present in the space environment.

3.3 Goal:

To successfully design and test an arcject thruster within a vacuum chamber that meets all of our customer's requirements.

3.4 Objectives:

- Operate on direct drive by eliminating the PPU
- Generate an arc capable of breaking down a gas propellant
- Produce a current density that will sustain the plasma
- Produce a model that is scalable for NASA applications
- Design and build a reliable test model
- Create a space-like test environment
- Create and carry out an experiment to determine the amount of thrust produced

3.5 Constraints:

- Work within our budget of $500
- Time constraints of deliverables
- Minimize weight
- Set input power source (Solar arrays provided by NASA)
- Produce a pressurized gas within a vacuum environment

4.0 Design and Analysis

4.1 Functional Analysis

4.1.1 Mechanical

4.1.1.1 Gas Valve Regulator

The gas valve regulator will be provided by the manufacturer of the argon gas tank and will function as a control valve to regulate the flow of argon gas into the thruster.

4.1.1.2 Thruster Housing

The thruster housing will function as the body of the thruster which houses some of the major components such as the annular anode, cathode, and magnets. The housing will also function as a control volume by containing the argon gas in order to allow for the plasma to be created.

4.1.1.3 Anode/Cathode Spacing

The anode and cathode spacing within the thruster housing will function as a major component in the arcjet thruster. The spacing between the anode and cathode is important because it determines the breakdown voltage needed to ionize the argon gas.

4.1.1.4 Nozzle

The converging-diverging nozzle within the arcjet thruster will allow the argon ions generated by the arc to be accelerated past sonic velocity. The nozzle will also function with the help of magnets to contain the plasma at a centerline off the walls of the nozzle.

4.1.1.5 Vacuum Chamber

The vacuum chamber will be used to house the arcjet thruster in order to conduct a proper experiment simulating the space environment, where the arcjet thruster will be used.

4.1.2 Electrical

4.1.2.1 Circuit

The circuit will consist of solar panels, an inductor, an IGBT, selector switch, and a potentiometer. The solar panels will provide electrical energy to the circuit and ionization process. The circuit must be capable of producing a voltage spike of at least 137 V and should also be able to reach a voltage of at least several hundred volts. Once the system is in steady state the current through the plasma (anode/cathode) should be approximately 5.5 A.

4.1.2.2 Magnets

The magnet is needed to direct flow of the plasma through the nozzle, protect the thruster from overheating, and help produce additional thrust.

4.2 Design Concepts

4.2.1 Mechanical

4.2.1.1 Design #1

The next design improves upon the design NASA previously produced in that it utilizes a converging-diverging nozzle in order to help accelerate the flow of the argon gas passed sonic velocity. Rather than injecting the argon gas directly through the cathode, this design injects the gas into the thruster housing perpendicular to the cathode. This design concept is depicted in Figure 1.

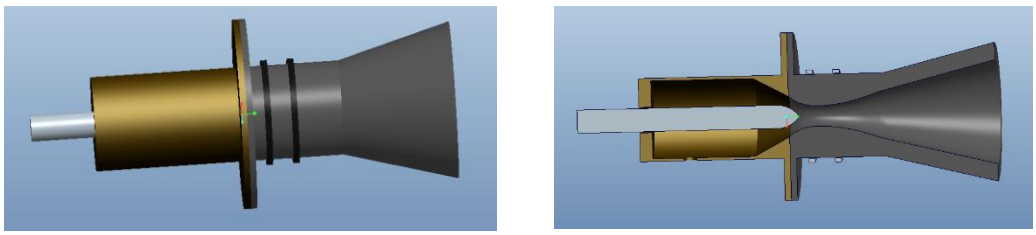

Figure 1: External and Cross-sectional View of Design 1

The converging diverging nozzle acts as the anode and the cylindrical rod with a pointed tip acts as the cathode. The magnets are placed around the front side of the nozzle and are represented as the rings in Fig. 1. The placement of the magnets will help confine the high temperature argon ions away from the surface of the nozzle and will help direct the flow downstream to the nozzle exit.

4.2.1.2 Design #2

The second arcjet thruster design is similar to Design 1 in that the argon gas is not directly injected into the cathode. Instead of injecting the gas into the housing perpendicular to the cathode, this design has the argon gas being injected into the housing at an angle. The reason for injecting the argon gas at angle is to create a convective flow of the argon gas that will help cool the cathode by creating a boundary layer. The CAD model of this design is shown in Figure 2.

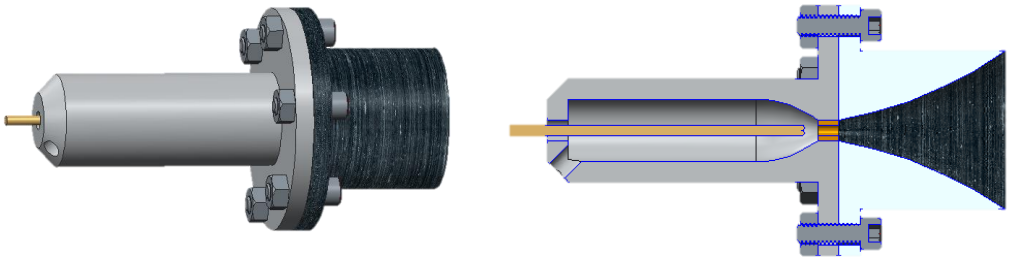

Figure 2: External and Cross-sectional View of Design 2

This design utilizes a cylindrical housing with the end of it acting as the converging portion of the converging diverging nozzle. The long cylindrical rod that is located along the centerline axis of the cylindrical housing is the cathode. The hole on the front side of the housing near the entrance of the cathode is angled in order to allow for the argon gas to be pumped into the housing as previously discussed. The anode is located at the end of the cylindrical housing inside the throat of the converging diverging nozzle. This will ensure that the arc between the cathode and anode will be generated when the argon gas is choked to sonic velocity. After the arc is produced the argon gas becomes ionized and is accelerated past sonic velocity. The argon ions are able to accelerate by increasing the area of the nozzle shown in Fig. 2 in the diverging portion. In order to attach the housing to the diverging portion of the nozzle, flanges are incorporated into the design of both parts. This will allow for ease of mating and securing the two parts together with the use of screws and nuts.

4.2.1.3 Design #3

The final design is very similar to Design 2 with insulation and machinability considerations taken into account. In order to attach the housing to the diverging portion of the nozzle, flanges are incorporated into the design of the housing chamber and the diverging nozzle. This will allow for ease of mating and securing the chamber, converging nozzle and diverging nozzle together with the use of screws and nuts.

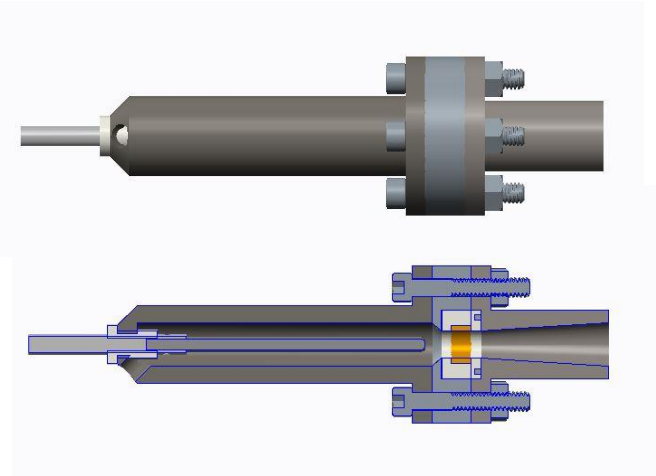

Figure 3: External and Cross-sectional View of Design 3

The design, shown in Figure 3, differs from Fig. 2 in several ways. A method of mounting the cathode was specified and involves threading the exterior and interior surfaces of a cylinder of insulation. This insulation is press fit into the far left of the chamber. One end of the cathode is also threaded and fits into the insulation, allowing for adjustability of the anode-cathode spacing.

Another aspect of the design that was found difficult to manufacture was the annular anode and its surrounding insulation. Since a wire must be fed through the insulation and flanges, the anode was designed to press-fit into one end of insulation. The wire can be attached to the anode, threaded through a clearance gap in the insulation, and an insulation "cap" bolted on to enclose the anode. The section created in Fig. 3 between the two flanges was also created in part for the clearance of the wire. In addition, this section was created to simplify the chamber's manufacturability such that the converging nozzle can be machined as a standalone piece. Upon analyzing the required area ratio in the diverging nozzle, Fig. 3 was also designed with a different nozzle shape, allowing for better manufacturability.

4.2.2 Electrical

4.2.2.1 Circuit

When the thruster is constructed, the actual anode/cathode spacing and pressure of Argon isn't accurately known. Since the breakdown voltage depends on the product of the pressure and anode/cathode distance, it is desired we design a circuit that can adjust the breakdown voltage to match the product of the pressure and distance. There are three different designs we could use to implement these requirements. Design 1 would be a power processing unit that converts the voltage and current to the proper value for thruster operation. The sponsor specifically asked us to replace this to make the system more efficient so that rules out that option. Design 2 is to create a voltage spike with a capacitive circuit, but the voltage

across a capacitor does not change instantaneously, so that would be difficult to do. A better design, Design 3, is to use an inductive circuit to create a voltage spike because the current through an inductor does not change instantaneously, however the voltage can. This is given by V = L$\frac{di}{dt}$, where di is the change in current, dt is the time it takes for the circuit to open, L is the inductance, and V is the voltage across the inductor. A functional schematic is shown in Figure 4. A potentiometer in place of R_2 is capable of adjusting the voltage spike, because steady state current will drop to zero in the amount of time it takes the IGBT to open, thus a potentiometer could control the di term, which controls the voltage spike.

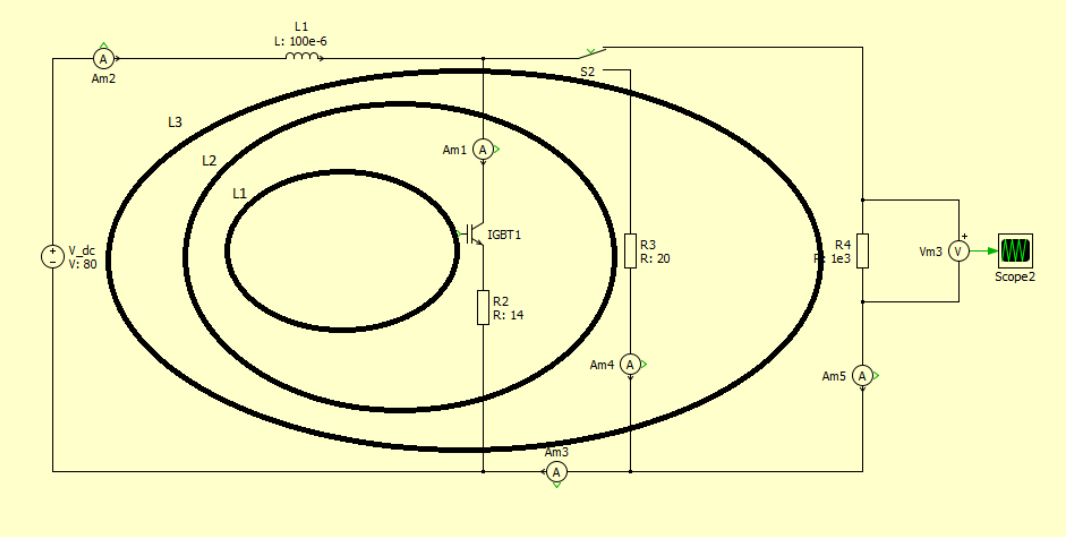

Figure 4: Circuit Design

In order to start up the thruster, the IGBT in Fig. 4 will be closed by a simple selector switch that provides enough voltage to close the IGBT. When the IGBT is closed, loop L1 will conduct current, while loop L2 and L3 will be open circuits. The time it takes L1 to reach steady state is given by $5 \times \tau = 5 \times \frac{L}{R2}$. We were unable to find a single potentiometer that had the range of resistance values required but could also handle the amount of current flowing through it and the amount of power dispersed so we are now going to use two potentiometers in series that each range from 0 to 200 ohms. An inductor was found that has an inductance value of 100 µH, thus τ has a maximum value of 40 ms and the minimum charge time (minimum duration of pulse across IGBT) is 0.2 s. When loop L1 reaches steady state the current will be $I_1 = \frac{V_{dc}}{R2}$, where V_{dc} is the voltage supply from the solar panel, thus I_1 will range from 0.2 A to 5.5 A. When the selector switch is opened the IGBT will open, hence every loop in Fig. 4 will be open, but the inductor will react strongly because the current through an inductor doesn't change instantaneously given by $V = L\frac{di}{dt}$, where dt is the IGBT flip time approximately 130 ns, L = 100 µH, di = I_1 – 0, hence the voltage spike will range from 153 V to

4230 kV. This breakdown voltage will create an arc across the anode/cathode gap shown in loop L3 as R_4 = 1 k Ω, which ionizes the argon flowing through the gap and produces a plasma. Immediately after the arc, current will flow through the plasma, which will act as a resistance that is unknown so we used 20 Ω for this particular simulation shown in Fig. 4, loop L2.

The report we received from our sponsor used four 100 W solar panels, two in series, and two in parallel, which outputs approximately 80 V and 5.5 A. We were also asked to produce the correct voltage spike if the solar panels are only outputting 40 V, which the thruster can do by simply adjusting the potentiometer. When we test the thruster in the lab we will use the power supply provided in the lab, but once the thruster is operating correctly, we will replace this power supply with the solar panels.

4.2.2.2 Magnets

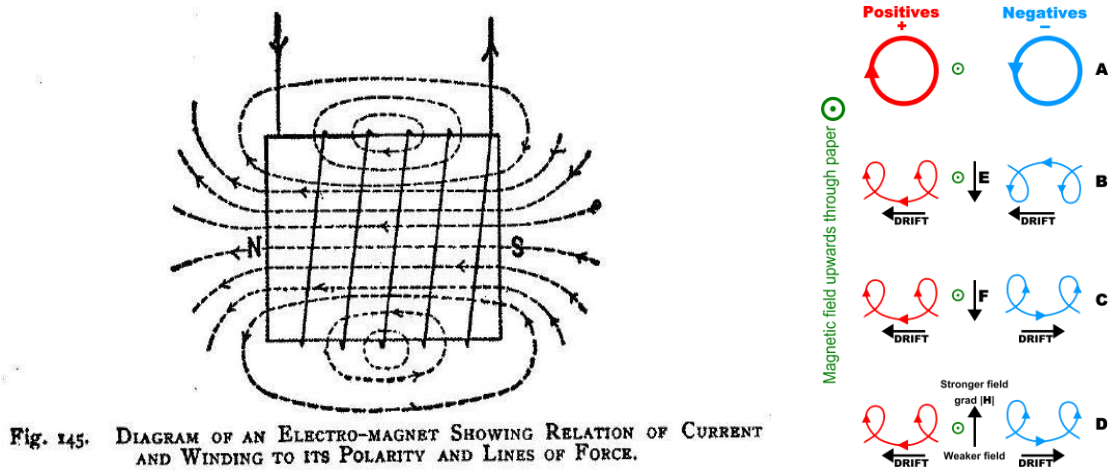

Figure 5: Magnetic Force Schematics

The magnet will be placed around the nozzle in order to keep the plasma off the walls of the nozzle and will confine the plasma to a certain radius. It also helps increase thrust. Figure 5 depicts an electro-magnet that can be replaced by a bar magnet with the same characteristics. One could imagine a plume of positive and negative charges due to the ionization of Argon through the anode/cathode. This plume wants to expand outward but the magnet is pushing the charges of the plume inward causing the charges to move in a helical path as shown in Fig. 5. The magnetic field at which we can confine the negative and positive charges in a bar magnet is given by B = $\frac{mv}{qr}$, where m is mass of argon ion, v is velocity of the argon ion, q is charge of a positive ion, r is the LARMOR radius (maximum radius of ion rotation), and B is the magnetic field. The mass of an argon ion is 6.683x10^(-26) kg. The typically velocity of ions expanding from a generated plasma field is equal to approximately 6925 m/s. The charge of an ion is approximately 1.673x10^(-19) C. The value of r will be equal to the size of the radius of the thruster at any point. After entering all those values and solving, the needed B field is found to be

approximately [3x10^(-3)]/r (T). The magnets were placed evenly so that each magnet was 0.022 meters apart. After choosing those locations, the necessary field strength that would be needed at those locations were determined to be 0.787 T, 0.360 T, and 0.313 T. After determining the necessary field strengths at each magnet location, it was necessary to derive equations for the total magnetic field at each of those locations due to the superposition of all three magnets and using the relation that magnetic field strength decays by $\frac{R^3}{(d^2+R^2)^{\frac{3}{2}}}$. After solving those three equations for the three variable magnet strengths, it was determined that magnet one should be 0.762 T, magnet 2 should be 0.238 T, and magnet 3 0.275 T. From this point, one can calculate the current needed to generate these fields by using the equation $I = 2RB/\mu_0$ if a single loop is used, or $I = B/n\mu_0$ for a solenoid where n is the number of turns per meter.

4.3 Evaluation of Designs and Selection of Optimum Ones

4.3.1 Mechanical

4.3.1.1 Evaluation of Designs

Table 1: Decision Matrix

		Design 1		Design 2		Design 3	
	Weights	Rating	Weighted Score	Rating	Weighted Score	Rating	Weighted Score
Life Expectancy	0.1	7.0	0.7	7.0	0.7	8.0	0.8
Material Cost	0.2	2.0	0.4	7.0	1.4	8.0	1.7
Ease of Assembly	0.1	6.0	0.6	8.0	0.8	3.0	0.3
Manufacturability	0.2	5.0	0.9	4.0	0.7	7.0	1.2
Ease of Closing Circuit	0.1	9.0	0.6	9.0	0.6	4.0	0.3
Temperature	0.1	8.0	1.1	4.0	0.6	9.0	1.2
Magnet Insertion	0.0	6.0	0.2	6.0	0.2	8.0	0.3
Gas Insertion	0.0	3.0	0.1	3.0	0.1	9.0	0.3
Reliability	0.1	2.0	0.3	7.0	1.0	8.0	1.1
TOTAL	1.0		4.9		6.1		7.2
RANK			**3**		**2**		**1**
Circuit		**Design 1**		**Design 2**		**Design 3**	
	Weights	Rating	Weighted Score	Rating	Weighted Score	Rating	Weighted Score
Reliability	0.4	1	0.4	6	2.4	10	4
Cost of Components	0.4	1	0.4	2	0.8	10	4
Simplicity	0.2	10	2	2	0.4	5	1
TOTAL			2.8		3.6		9
RANK			**3**		**2**		**1**

The detailed matrix chart, shown in Table 1, was used as an aid in deciding which design best suited the needs of the project. Each design was measured in its ability to fulfill a total of nine different categories: life expectancy, material cost, ease of assembly, manufacturability, ease of closing the circuit, temperature, magnet insertion, gas insertion and reliability. These categories were given a weight based on the influential importance each would have on the desired final product –

the sum of all categories adding up to 1, such that a weighted score could be assigned to each design. Based on the ratings given to each design, a final weighed score is established such that the higher the final total, the more desirable the design.

Designs 1 and 2 fell short for a variety of reasons. Design 1 scored low in reliability since the flow of fuel through the arc isn't maximized as it is in the other two designs. The cost of the first design is also significantly higher due to the selection of an expensive insulation material to be used between the cathode and the grounded material.

As a result of this decision matrix, Design 3 was determined to be the best option. It scored the highest in seven of the nine categories, falling short in its ease of assembly and ease of closing the circuit. This design calls for the magnet to be placed in the throat of the system in addition to being wrapped around the exterior of the nozzle. Changes made from Design 2 to Design 3 allow the machinability and assembly to be made drastically easier.

Conversely, this design scored very high in gas insertion method and temperature control. Design 1 injects the fuel in a direction parallel to the desired thrust direction, Designs 2 and 3 deposit the fuel at an angle to the final flow direction. This creates swirls which aid in cooling the high temperature fuel and potentially exposing a higher percentage of gas to the electric arc.

4.3.1.2 Final Design

Of the three designs, the arcjet thruster that best suited the customer needs was found to be that shown in Fig. 3. Instead of injecting the gas into the housing perpendicular to the cathode, this design has the argon gas being injected into the housing at an angle. The reason for injecting the argon gas at angle is to create a convective flow of the argon gas that will help cool the cathode by creating a boundary layer.

This design utilizes a cylindrical housing with the end of it acting as the converging portion of the converging diverging nozzle. The long cylindrical rod that is located along the centerline axis of the cylindrical housing is the cathode. The hole on the front side of the housing near the entrance of the cathode is angled in order to allow for the argon gas to be pumped into the housing as previously discussed. The anode is located at the end of the cylindrical housing inside the throat of the converging diverging nozzle. This will ensure that the arc between the cathode and anode will be generated when the argon gas is choked to sonic velocity. After the arc is produced the argon gas becomes ionized and is accelerated past sonic velocity. The argon ions are able to accelerate by increasing the area of the nozzle shown in Fig. 1 in the diverging portion. In order to attach the housing to the diverging portion of the nozzle, flanges are incorporated into the design of both parts. This will allow for ease of mating and securing the two parts together with the use of screws and nuts.

5.0 Risk and Reliability Assessment

The major risk involved in our project is the melting of our internal components due to the exposure of high temperatures. The way this risk has been mitigated is by using high temperature resistant materials such as tungsten and stainless steel, as well as the use of magnets to confine the high temperature plasma away from the inner walls. Another risk involved is unsuccessfully grounding the annular anode and cathode. This risk will be avoided by using a Macor insulation to make sure the charged materials are grounded. A risk of ionizing the plasma prior to the throat of the nozzle has also been taken into account. In order to reduce this risk the throat distance has been designed to be closest to the cathode.

6.0 Detailed Design and Design for Manufacturing

Please see Appendix A for detailed CAD drawings for the main parts of the thruster design.

All of our major components have been approved by the head FSU machine shop machinist, Jeremy, therefore the components are easily machinable using standard machine shop equipment.

7.0 Procurement and Budget

Table 2: Budget Allocation Request

Component	Description	Quantity	Cost	Manufacturer
Cathode	Tungsten Rod, 3/16" x 6" P#8788A153	2	$ 33.24	McMaster Carr
	Stainless Steel 303, 3/16" x 6' P#8984K93	1	$ 7.77	McMaster Carr
Anode	SS Steel Tube 1/2 OD, 0.37 ID 3' P# 9220K461	1	$ 8.79	McMaster Carr
Argon Gas Cylinder	20 CF, Welding Cylinder	1	$ 77.00	Welding Supplies from IOC
Argon Gas	20 CF Fill	1	TBD	TBD
Hose from Arcjet to Baseplate	Air and Water Hose 1' P# 5304K9	1	$ 13.97	McMaster Carr
Hose Fitting to Arcjet	ARO-Shape Hose Coupling P# 5343K74	1	$ 12.90	McMaster Carr
Fitting to Arcjet Fitting	Industiral Shape Hose Coupling P# 6534K72	1	$ 4.21	McMaster Carr
Hose Fitting to Baseplate	Through-Wall Coupling P# 50785K274	1	$ 11.23	McMaster Carr
Hose Fitting from Baseplate Fitting	Female Barbed Hose Fitting P# 5346K72	1	$ 9.20	McMaster Carr
Hose	1" x 5' Hose P#5304K45	1	$ 12.65	McMaster Carr
Housing/Nozzle	Stainless Steel 303, 2' Diameter, Stock P#8984K573	1	$ 79.64	McMaster Carr
Gasket	All Purpose Sheet Gasket 6"x6" P# 9470K26	2	$ 6.02	McMaster Carr
Bolts (Anode)	P# 92185A078	1	$ 3.23	McMaster Carr
Mating Bolts	P# 92185A546	1	$ 5.43	McMaster Carr
Nuts for Mating Bolts	P# 91845A029	1	$ 4.57	McMaster Carr
Insulation	Macor Rod P#8489K81	1	$ 72.95	McMaster Carr
IGBT	Part# IRG7PH30K10DPBF	1	$ 8.73	Digi-Key
Inductor	100.0 µH, 6 A PART#1410460C	1	$ 2.62	Digi-Key
Switch	PART# C3900BA	2	$ 8.92	Digi-Key
Potentiometer	Part# AVT20020E200R0KE	2	$ 31.24	Digi-Key
Magnet	Ceramic Ring Magnet, ID 2"	3	$ 11.25	American Science & Surplus
Spring	Extension Spring #EBD-012-672-S	2	$ 7.50	The D. R. Templeman Company
		TOTAL	**$ 433.06**	

As previously mentioned, the budget for this project is set at $500. Table 2 shows the current projected expenditures totaling $433.06. This leaves a slight financial cushion in the event that any parts fail or require modifications in machining. Not listed above is the machining requirements for the vacuum chamber. Therefore, a portion of the leftover budget will be used in manufacturing the baseplate. This expense is not included in the above table as the current vacuum chamber design has not been finalized due to a projected insufficient back pressure.

8.0 Communications

Our team communicates effectively with each other, our advisors, and sponsor. We make the most of our meeting times and are efficient with our meetings. We set up meetings and conference calls with our advisors and sponsor about every two weeks. Our group meets once to twice a week depending on the work load and requirements of the project. We use email, text messaging, twitter, and phone calls to communicate information about project deadlines and plans.

9.0 Conclusions

Elimination of the power processing unit as demonstrated in our choice of Design 3 would, theoretically, allow for sufficient thrust at a reduced cost for spacecraft propulsion. In addition, lifetime of the system is increased since failure of PPU is no longer in consideration. Price of the general design is also significantly diminished by using direct-drive, as current designs must allocate a large portion of the budget to invest in a power processing unit.

As mentioned above, a major expenditure for the project is derived from the need to manufacture a vacuum chamber specifically for testing purposes. Had this design been implemented and tested in a facility already possessing a viable vacuum chamber, the costs of this project would be greatly reduced. Taking this into account, the overall expenses for a design such as this provides a better opportunity to meet the customer's budget of $500.

The design chosen should effectively capture the opportunity to both provide thrust with magnetic acceleration of ionized particles and thermal expansion of argon gas and plasma. The design that is planned to be implemented should prove to be easy to manufacture and adjust when conditions arise. However, issues still exist and will need to be ironed out during the testing phase of the project and will be discussed further in Future Plans.

10.0 Environmental and Safety Issues and Ethics

Some safety issues with ion arcjet thrusters are if not fully knowledgeable about how it works, one could severely injure or possibly kill themself. One reason is because the thruster produces high voltage, which can be harmful especially if it travels across your heart. Another safety issue is asphyxiation from Argon while testing. Also, the vacuum pump can possibly create too much suction on the bell jar and shatter it. The heat produced by the thruster could potentially melt the glass bell jar.

11.0 Future Plans for Prototype

Future plans for the prototype include verifying prototype design with sponsor, Dr. Polzin, prior to ordering materials needed. Upon approval of the design, a purchase order will be submitted through AME so that the components will arrive prior to the beginning of the spring semester. Once materials and components are received, CAD drawings will be finalized and submitted to the FSU machine shop for fabrication. During this fabrication phase, the electrical components will be tested in lab to verify voltage spike. Further into the spring semester, a

testing plan and testing apparatus will be developed to quantify the operational range of the thruster and circuit along with measuring the output thrust. Once a testing plan is developed and a suitable vacuum chamber is obtained, the experiment will be performed, analyzed, and iterated. Upon multiple successful experiments, the group would like to travel to the Marshal Space Flight Center in Huntsville, Alabama in order to test our design inside their vacuum chamber and integrate the solar panels.

12.0 Gantt Chart, Resources, Budget

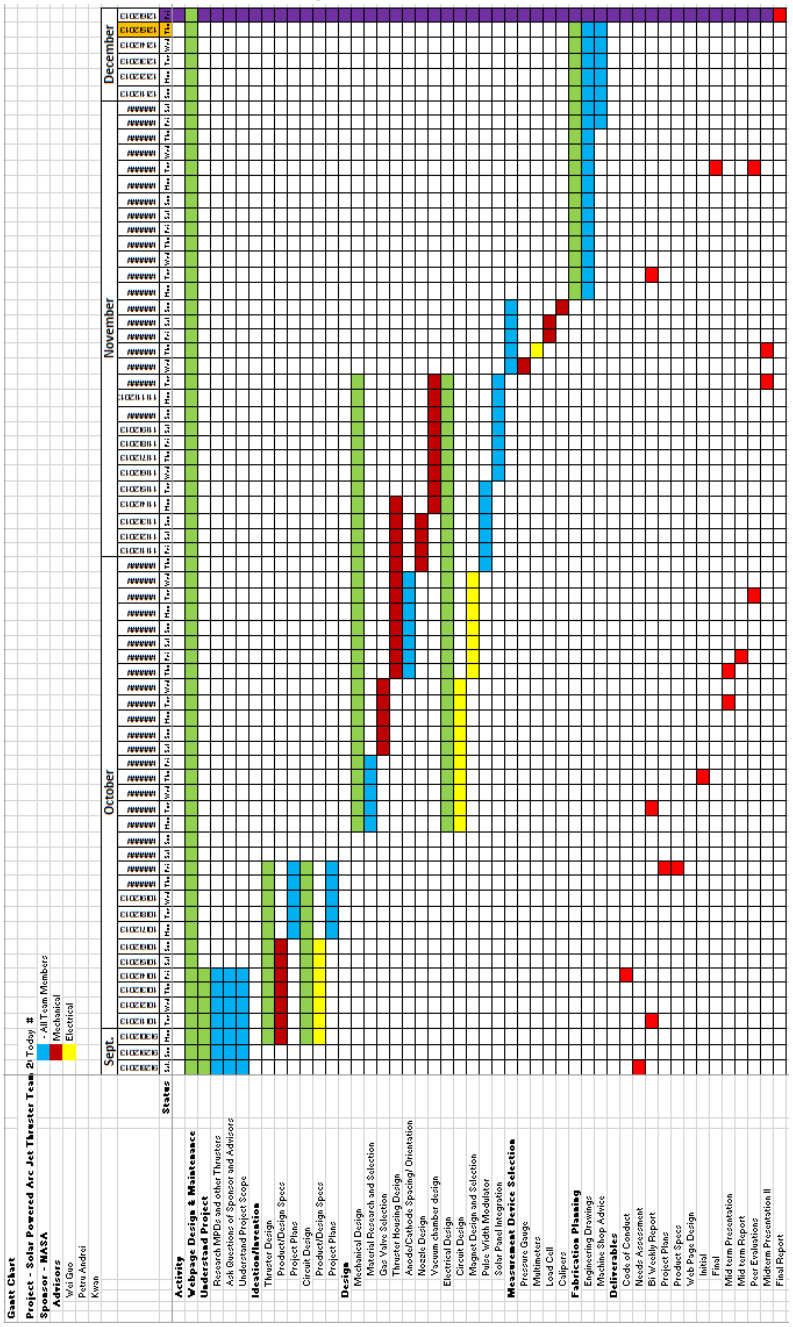

13.0 References

1) Polzin, Kurt. "Senior Design Project Definition." NASA, n.d. Web. 26 Sept. 2013.
2) Matthew Krolak. “MPD Thruster Thesis.” Worcester Polytechnic Institute, May 2007.
3) Nicolas Augustus Rongione. “Direct Solar Powered Arcjet Thruster (DiSPAT)” NASA, n.d. August 9, 2013.
4) William Anthony Hargus, Jr. “Hall Acceleration Mechanism” US Air Force Research Laboratory. March 2001
5) Geoff Dickinson. “Non-impulsive orbit raising using an ATOS type arcjet thruster” ASEN5050. Dec. 2002.
6) F. Paganucci, P. Rossetti, M. Andrenucci. “Performance of an Applied Field MPD Thruster” RIAME-MAI. 2001.

Appendix A – Mechanical Detailed Design

Detailed Product Specifications

Please find attached detailed engineering drawings for all the components of the thruster. The thruster consists of nine main parts, with other gaskets, bolts, and nuts.

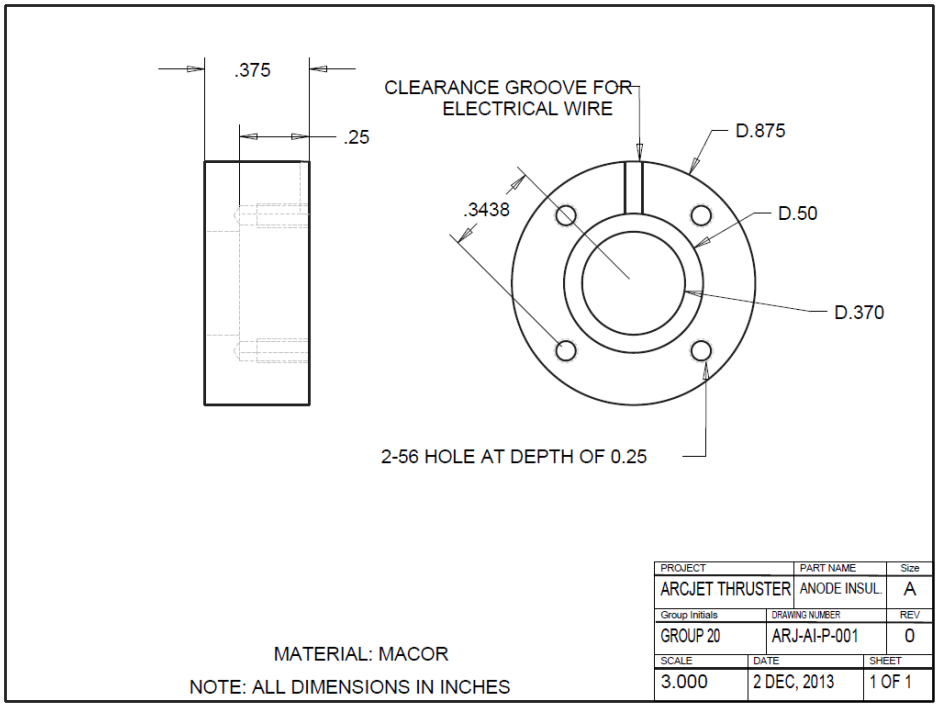

Figure A. 1: Anode Insulation Drawing

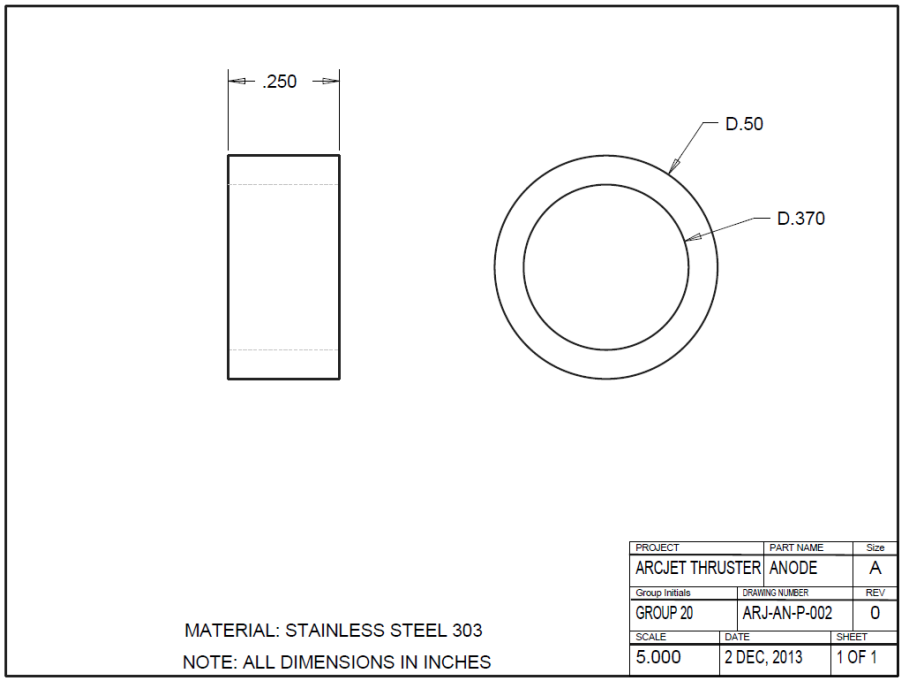

Figure A. 2: Anode Drawing

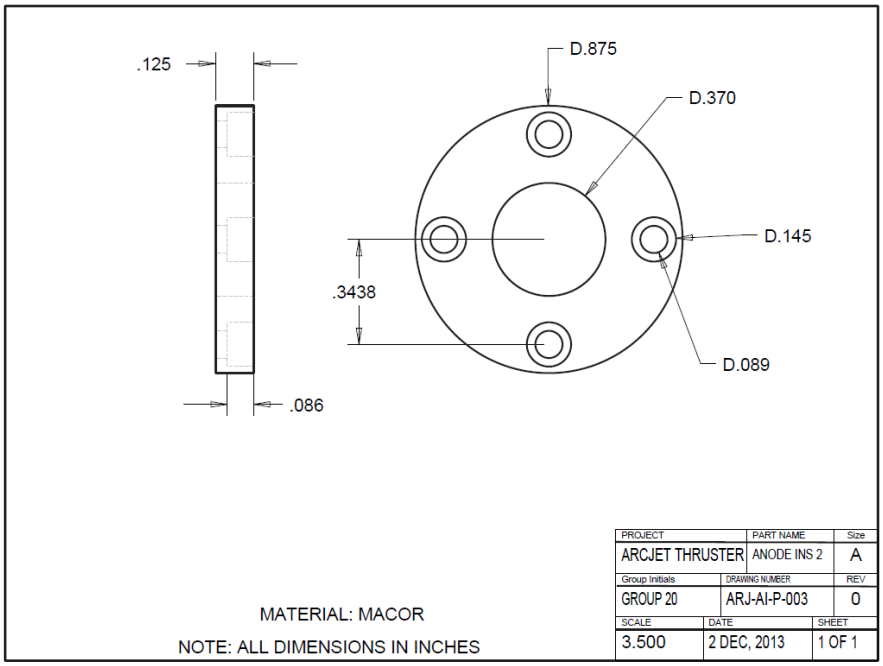

Figure A. 3: Anode Insulation 2

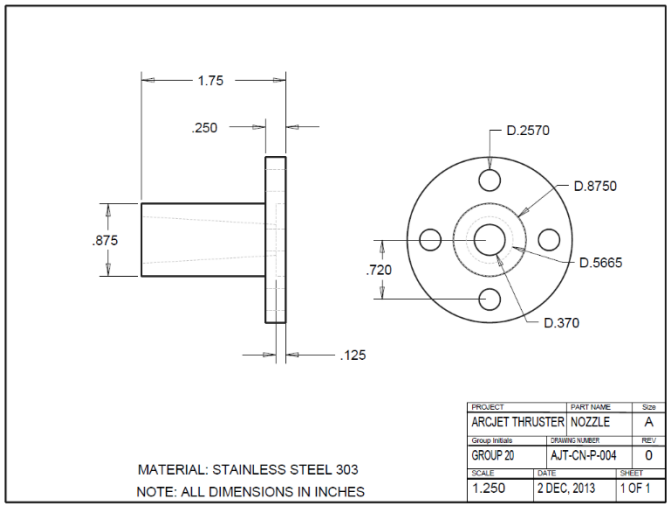

Figure A. 4: Nozzle Drawing

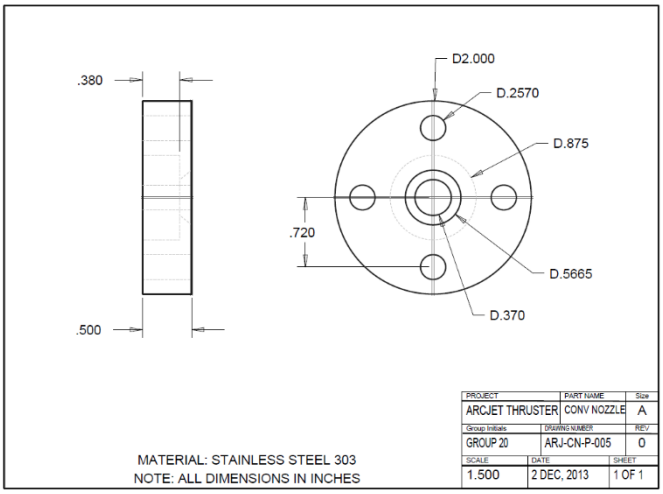

Figure A. 5: Converging Nozzle Drawing

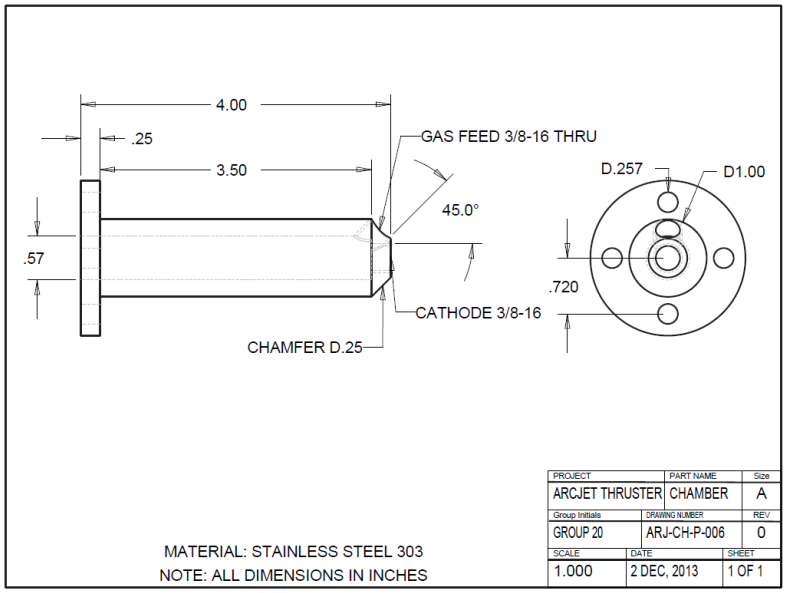

Figure A. 6: Chamber Drawing

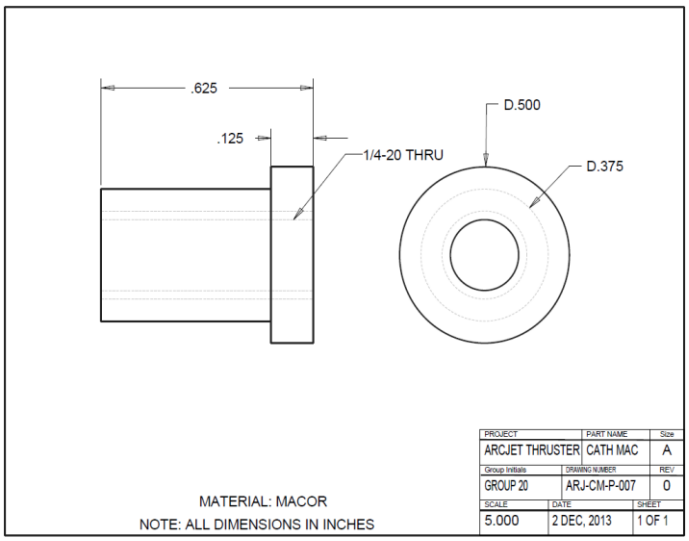

Figure A. 7: Cathode Macor Drawing

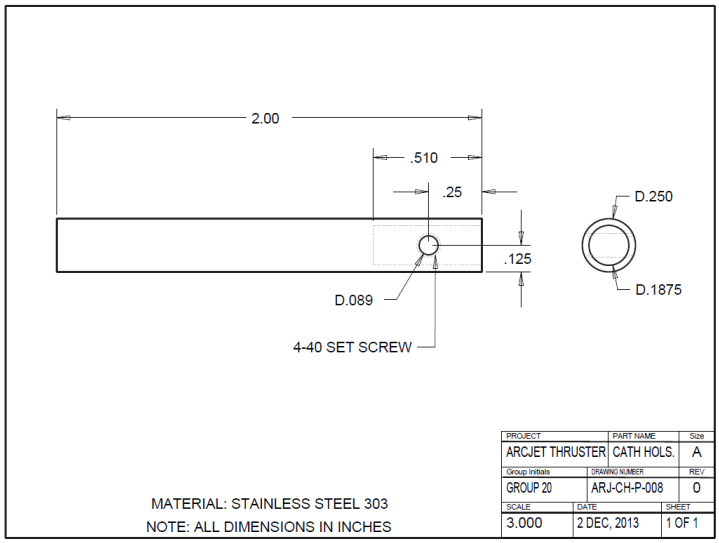

Figure A. 8: Cathode Holster Drawing

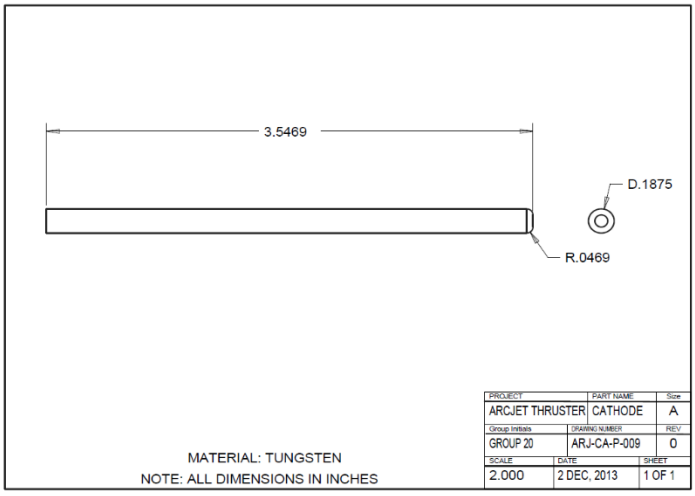

Figure A. 9: Cathode Drawing

Appendix B – Electrical Detailed Design

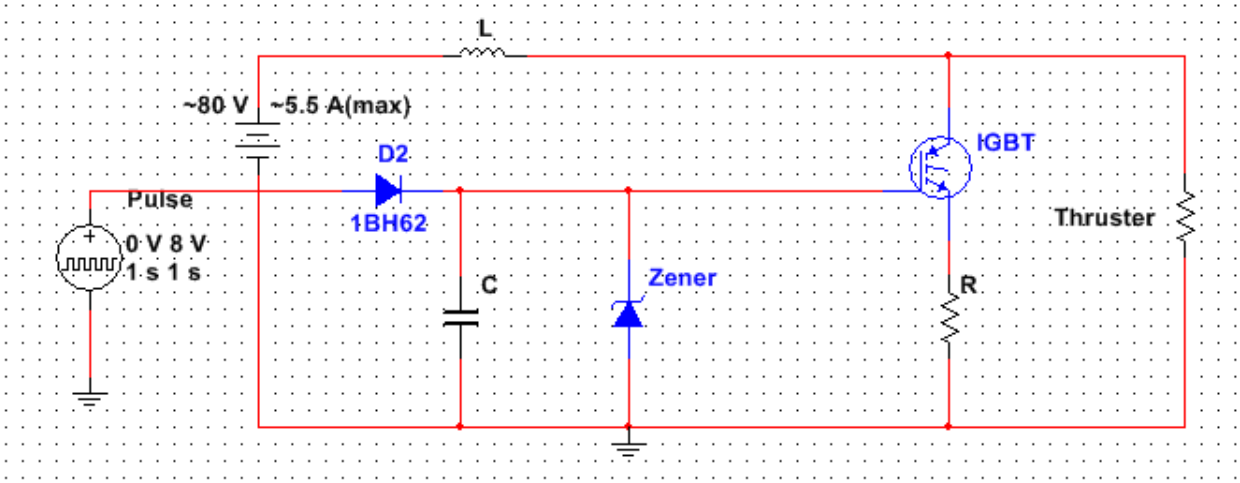

Figure B. 1: Electrical Design

Figure B.1 is a detailed design of a functional circuit that meets the requirements. The magnet design will look similar to Figure B.2.

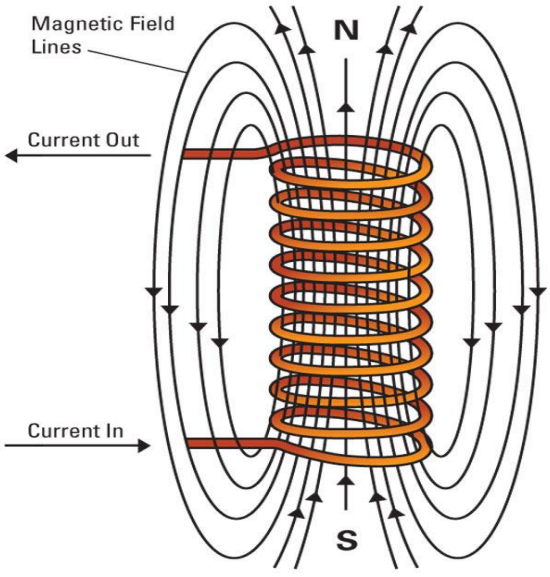

Figure B. 2: Magnetic Design

The figure above depicts an electromagnet that will be similar to the one we test with the thruster. The number of turns and current will determine the magnetic field strength, and we will replace the electromagnet with a permanent magnet.

Appendix C – Finite Element Modeling

Calculations

14.3.1 Mechanical

```
%Feed Calculations

P_o = [2500:-1:500]; % Stagnation Pressure in the Cylinder (psi)
P_o2 = P_o.*6894.76; % Stagnation Pressure in the Cylinder (Pa)

P_g = 20; % Static Pressure leaving Cylinder (psi)
P_g2 = P_g*6894.76; % Static Pressure leaving Cylinder (Pa)

rho_argon = 1.784; % kg/m^3
D_feed_tube = 0.25*0.0254; % Diameter of the Gas feed tube in (m)

D_Throat = 0.75*.0254; % Diameter of nozzle throat (m)
A_Throat = (3.1416/4).*(D_Throat.^2);
P_c = 245.31:.3773:1000; % Ionization Chamber Pressure (Pa)
d = 0.00381; % Anode-Cathode distance (m)
P_v = (1*10^-4)*133.322368; % Ambient Pressure of Vacuum Chamber (Pa)

% Canister to Feed Tube
V_g = sqrt(2*rho_argon.*(P_o2 - P_g2));%m/s
    m_dot_Ar = V_g.*(rho_argon*3.1416*((D_feed_tube)^2)/4); % kg/s

% Feed tube to Ionization Chamber
V_c = sqrt((P_g2 - P_c) + (0.5*rho_argon.*V_g.^2).*2*rho_argon); %m/s
    A_Ion = m_dot_Ar./(V_c.*rho_argon); %m^2
    V_Ion = A_Ion.*(8*.0254); % Volume of the Ionization Chamber

% Velocity Exiting the throat
V_v = sqrt((P_c - P_v) + (0.5*rho_argon.*V_c.^2).*(rho_argon*2)); %m/s
    m_dot_exit = V_v.*(rho_argon.*A_Throat);% kg/s
    %A_Throat = m_dot_Ar./(V_v.*rho_argon); % m^2

subplot(1,3,1)
plot((P_g2./P_o2)./1000,m_dot_Ar, 'r')
title('Mass Flow Rate of Argon into Chamber')
xlabel('Static Pressure/Stagnation Pressure in Feed Tube(ND)')
ylabel('Mass Flow Rate (kg/s)')

subplot(1,3,2)
plot(P_c./1000,V_Ion.*(100^3),'--b')
title('Volume of Ionization Chamber vs Chamber Pressure')
xlabel('Ionization Chamber Pressure (kPa)')
ylabel('Chamber Volume (cm^3)')

subplot(1,3,3)
plot((P_g2./P_o2)./1000,V_v,'--r')
title('Static/Stagnation Pressure vs Exit Velocity ')
```

```
xlabel('Static/Stagnation Pressure (ND)')ylabel('Throat Exit Velocity (m/s)')
```

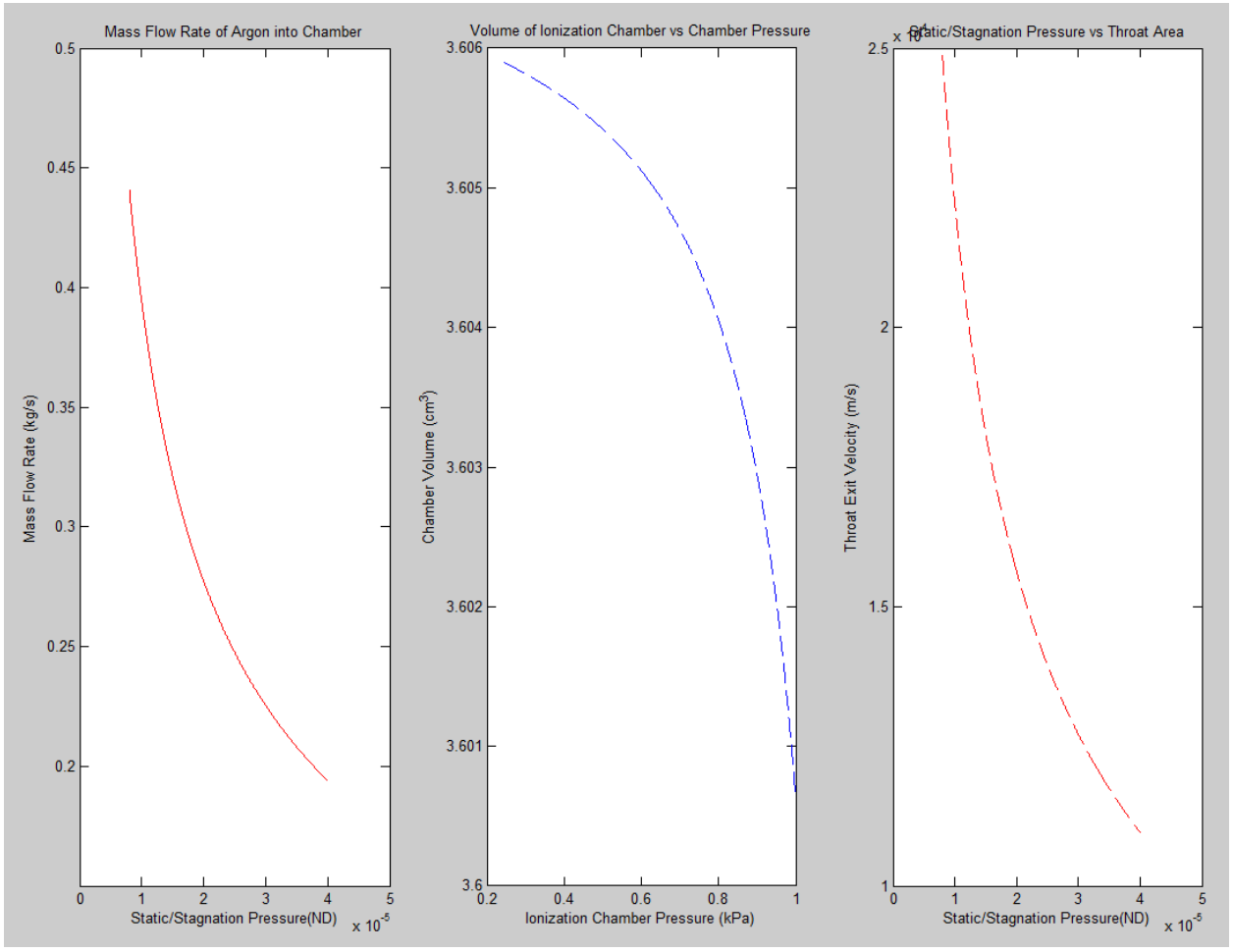

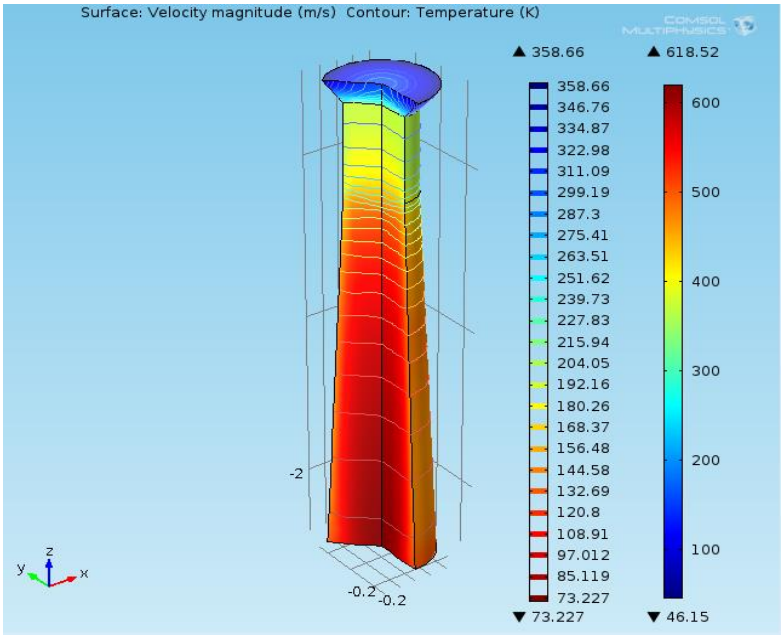

Appendix D – Electrical Calculations

For the magnet we attempted to calculate the magnetic field using $B = \frac{mv}{qr}$, $v = \sqrt{\frac{20eV}{3m}}$. These equations combine to give us B = 790 mT.

.

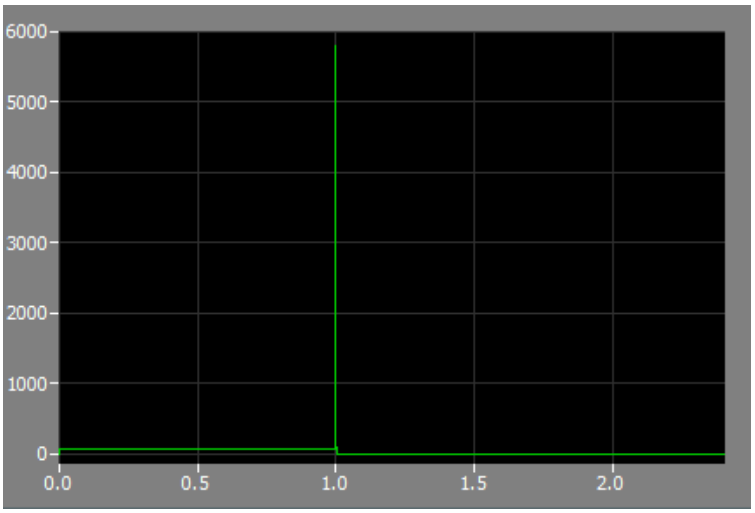

We simulated Fig. 4 in section 4.2.2.1 and produced the voltage spike shown in the figure above. This voltage spike is higher than anticipated, but we simulated many times using different resistor values and we would get some voltage spikes in the order of 10^9 V. These were obviously wrong, but this particular simulation gave a voltage spike at 5.9 kV, slightly more intuitive. The reason the voltage spike is higher than anticipated is because MATLAB uses ideal IGBTs meaning the dt term is extremely small yielding a large voltage spike. There is a way to use a non-ideal IGBT in MATLAB, but the simulation ran for hours and eventually crashed every time we ran it. We also ran the simulation in MultiSim, but didn't get any voltage spike at all.